On the Behaviour of Hydrodynamic Processes due to the Presence of Submarine Sand Waves

Ingo HENNINGS[1], Blandine LURIN[1], C. VERNEMMEN[2], and U. VANHESSCHE[2]

[1]GEOMAR - Forschungszentrum für marine Geowissenschaften der Christian-Albrechts-Universität zu Kiel
Wischhofstrasse 1-3, D-24148 Kiel, Germany
Tel.: (49)4316002312 - Fax: (49)4316002926
e-mail: ihennings@geomar.de

[2]Laboratory of Physical Geography Research Unit for Marine and Coastal Geomorphology (RUMACOG)
University of Gent, Krijgslaan 281, S8, B-9000 Gent, Belgium
Tel.: (32)92644767 - Fax: (32)92644970
e-mail: carlos@selifa.rug.ac.be

Abstract

Radar signatures of the sea bed in coastal waters show that submarine sand waves superimposed on sandbanks or tidal current ridges change their orientation and character abruptly at the crest of the ridge. These observations were made when studying air- and spaceborne radar images of the southern North Sea (McLeish et al., 1981). Similar phenomena were already reported by analysing side-scan sonar records from the large sandbanks in the North Sea (Houbolt, 1968). Such observations could be evidence for changes of tidal current direction as the tidal flow approaches the crest of the sand ridge. Sand waves are flow-transverse bedforms which are oriented more or less perpendicular to the maximum tidal current velocity. Furthermore, several side-scan sonar records reveal megaripples on both sides of sand waves. The ripple height generally increases in the direction of the sand wave crest. Side-scan sonar records also reveal that the crestlines of megaripples in the troughs as well as on both sides of the slopes of the sand waves form a maximum angle of 45^0 with the crestline of the sand waves itself. The existence of such an angle between the crestline of megaripples and sand waves indicates that changes of the tidal current direction across sand waves can be expected. Direct evidence that such tidal current direction changes occur above sand waves is derived from measurements of the Air-Sea Interaction Drift Buoy (ASIB) system at the sea surface and from side-scan sonar records of the sea bed. Both systems were operated from on board research vessels during two C-STAR field experiments in the Hoek van Holland study area off the Dutch coast in April 1996 and in April 1997. Measurements performed by electrical resistance wires on board the ASIB system indicate that variations of the short and moderate wave direction and the wave directional spread are associated with changes of the tidal current direction at the sea surface. According to the results of the measurements derived from the ASIB system and the side-scan sonar records it can be summarized that the variation of the direction of short and moderate period water waves as well as changes of the tidal current direction across large sand waves must be considered for correct modelling of the wave-current interaction mechanism.

Introduction

One of the major challenges of morphodynamic modelling is to investigate the different scale interactions of tidal current ridges, sand waves, and (mega) ripples (De Vriend, 1997). Field et al. (1981) published a hierarchy of superimposed bedforms on a sandbank ranging from linguoid (mega) ripples (spacing: < 1 m), small sand waves (spacing: 10 - 20 m) up to large sand waves (spacing: 200 - 500 m). An overview of spatial scales of bedforms and ocean floor topography as a function of water depth by using different remote sensing radar systems was presented by Hennings (1998). Imaging radars are used for detecting tidal current ridges, sand waves, and other morphological changes of the sea floor in water depths $\leq$ 50 m (Alpers and Hennings, 1984; Shuchman et al., 1985; Vogelzang et al., 1997). Radar images of sea bottom topography confirm that sand waves, as they approach the crest of a tidal current ridge, do not maintain their crestlines at approximately normal to the general direction of peak tidal flow but bend around to become tangential to the crest of the ridge. Real Aperture Radar (RAR) images of the southern North Sea analysed by McLeish et al. (1981) show that sand waves which are superimposed on tidal current ridges change orientation and character abruptly at the crest. Similar phenomena from the large sandbanks in the North Sea were earlier reported by Houbolt (1968). McLeish et al. (1981) showed a K_a-band RAR image of the Schouwenbank of the Zeeland Ridges off the Dutch coast in the southern North Sea from December 8, 1979, 12.19 UTC. This radar image shows that the sand waves of the gentle southeastern slope of the Schouwenbank are arcuate, concave to the southwest. This could be evidence that the tidal current direction

changes if the tidal flow approaches the crest of the ridge, because sand waves are flow-transverse bedforms which are oriented more or less perpendicular to the peak tidal current flow. Several other side-scan sonar records of the southern North Sea reveal that megaripples are also present on both sides of the sand waves (Terwindt, 1971). The ripple height generally increases in the direction of the sand wave crest. The crestlines of the megaripples in the troughs and on both slopes of the sand waves form an angle α with the crestline of the sand waves. The angle α may reach values up to 45^0 and it seems to be a function of the sand wave slope. Langhorne (1973) showed that small dune bedforms are often oriented at considerable angles to the crestlines of sand waves. Field et al. (1981) presented small sand waves (height: 1 m; spacing: 20 m) oriented at a small oblique angle on the stoss slopes of large sand waves (height: 2 m; spacing: 200 m). The existence of an angle between the crestline of megaripples and sand waves may indicate that the direction of tidal currents also changes across sand waves.
Direct evidence that changes of tidal current direction occur above sand waves has been obtained from side-scan sonar records (see section 1) and from measurements derived by the Air-Sea Interaction Drift Buoy (ASIB) system (see section 2) in the C-STAR study area. Finally, the conclusion will be presented.

1-Bathymetry and side-scan sonar data

During the field experiment of the "Coastal Sediment Transport Assessment using SAR imagery (C-STAR)" project of the Marine Science and Technology (MAST-III) programme of the European Commission (EC) one measurement campaign was carried out during April 6-11, 1997, in the C-STAR study area by the University of Gent, Research Unit for Marine and Coastal Geomorphology (RUMACOG), Gent, Belgium. The main purpose of the measurement campaign was to explain bathymetric evolutions, to improve the quality of the existing data base and to expand the dataset with more precise and relevant side-scan sonar and grabs data. The study area is located in the southern North Sea, 30 km northwest of Hoek van Holland, The Netherlands, indicated by a circle in the inset of Fig. 1. The bathymetry of the 5 km by 5 km test site is presented in Fig. 1. Track 9 of the Air-Sea-Interaction Drift Buoy (ASIB) system (see section 2) and the track of the side-scan sonar system are also indicated in Fig. 1.
The study area shown in Fig. 1 has an average water depth of 27 m, a minimum water depth of 18 m, and a maximum water depth of 31 m and is covered by large sand waves. In the eastern and southeastern regions of the study area, the mean horizontal spacing of sand waves is 560 m with a maximum spacing of 900 m. To the west, the distribution of sand waves is more dense and the mean spacing decreases to 430 m. The southeastern region is characterised by a less dense pattern of sand waves. Only 5 transverse bedforms were observed in this subarea of 2 km x 2 km indicated by a black square in Fig. 1. The mean spacing of the sand waves in this subarea is 500 m and the maximum value is 1000 m. The sand waves are of the progressive type (Van Veen, 1935) formed by dominating flood tidal currents. Consequently, the gentle slope of the sand waves is oriented towards the northeasterly (NE) direction of the flood tide, while the steep slope is in the direction to the southwesterly (SW) ebb tidal current. In other words, the steep side of the asymmetric sand waves is at the NE side and the gentle side is towards the SW. The sand waves are not perpendicular to the dominant northeasterly flood-tidal current. Measurements of the tidal current direction (see section 2) show that the sand waves occur at an average angle of 10^0-15^0 to the dominant tidal current direction. An important feature determined on the bathymetric map (see Fig. 1) is the inclination of the sea floor. The inner shelf floor deepens to the west and northwest. Different patterns or shapes of sand waves can be observed in the study area. The southeastern subarea is dominated by sand waves with almost straight crests, while the shape of the crests evolves to a more sinuous form in the western subarea. In other words, the crest alignement changes from two-dimensional to three-dimensional patterns. Also, the number of sand waves per unit surface area increases to the west.
There are at least two main reasons why the orientation of the sand waves shows a small clockwise angle of 10^0-15^0 to the mean direction of the flood tidal current: 1. the sand waves are relict forms or 2. the height and volume of the transverse structures have a deviating influence on the mean current direction.
Megaripples are small scale bedforms (height: 0.5 - 1.5 m; spacing: < 20 m) and are a product of the peak tidal currents (Lanckneus et al., 1994). In other words, these transverse bedforms fluctuate in position, shape, and size, depending on the strength, direction and type of the current present. Megaripples tend to increase in size towards the top of sand waves.
A digital dual-channel Klein Model 595 side-scan sonar was used to record the seabed topography along a total of 21 tracks in the southeastern subarea of the C-STAR study site. Two examples of 500 kHz side-scan sonar images taken during a northeast to southwest track are shown in Figs. 2a-b. Both locations of the side-scan sonar images are indicated as sss-02-b/1 and sss-02-b/2 in Fig. 1. These two side-scan sonar images were recorded on April 08, 1997 during 09.01 - 09.15 UTC at a peak southwesterly ebb tidal current velocity of 0.95 ms^{-1}. The

recorded sea bed covers an area of about 75 m in range direction on both sides perpendicular to the track of the side-scan sonar fish. The megaripples seem to develop dominantly on the gentle slopes of the sand waves, but Fig. 2b shows that megaripples are also present on the steep slope of the sand wave. Almost straight linear crests with several bifurcations close to the crest of the sand wave are indicated on the side-scan sonar images. The relative heights of the megaripples decrease towards the trough of the gentle slope of the sand wave. The angle between the sand wave crests and the megaripple crests near the top of the sand waves is approximately 15^0. Lanckneus et al. (1994) showed that the megaripples have an orientation perpendicular to the peak (tidal) currents.

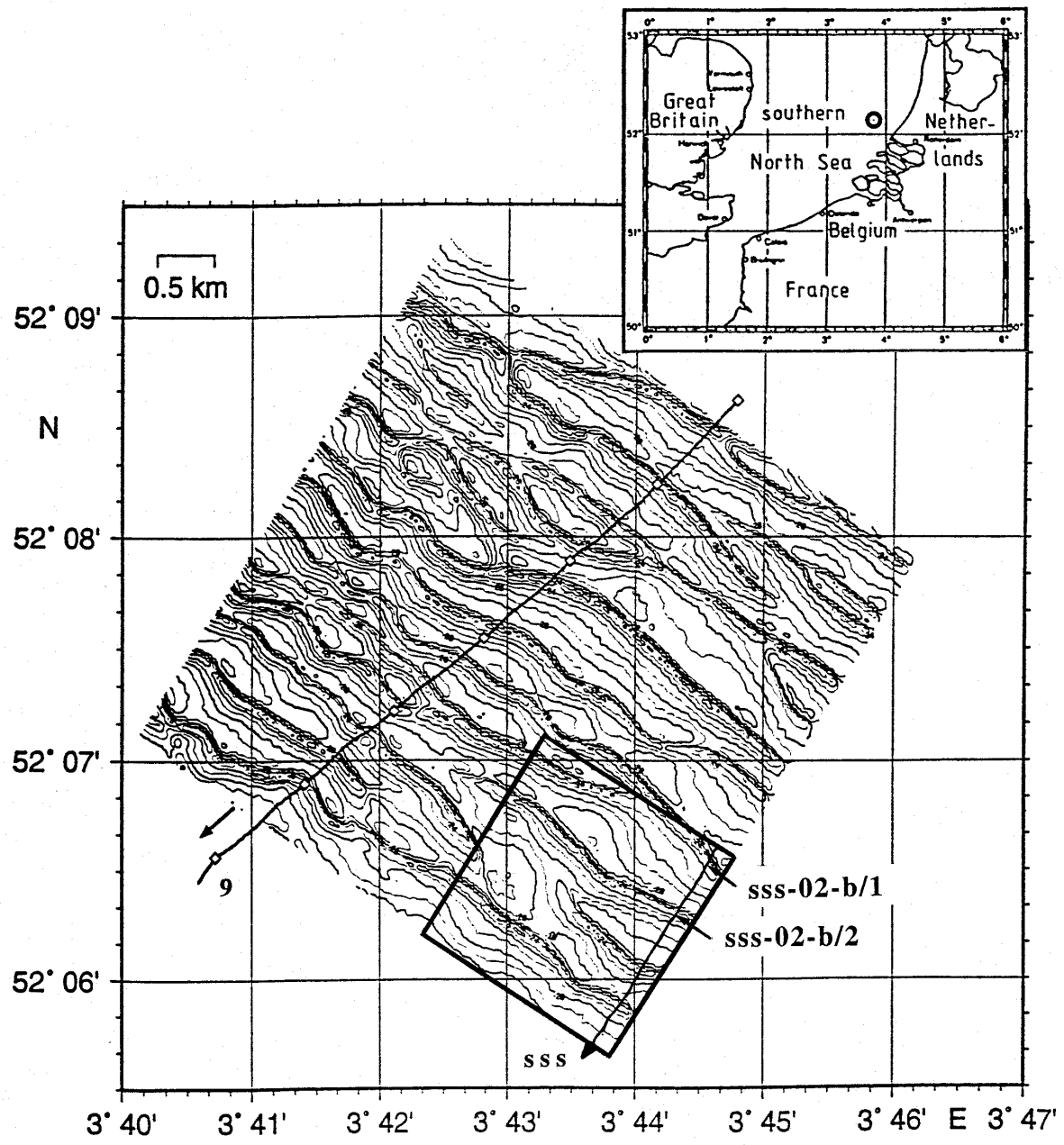

Fig. 1. Bathymetric chart of the C-STAR study area Hoek van Holland. Track 9 of the Air-Sea-Interaction Drift Buoy (ASIB) system and the side-scan sonar track (sss) as well as the locations of the two analysed side-scan sonar images sss-02-b/1 and sss-02-b/2 are also indicated. The 2 km x 2 km analysed subarea is marked by a black square at the southeasterly region of the bathymetric map. The study area is located in the southern North Sea indicated by a circle in the inset of Fig. 1.

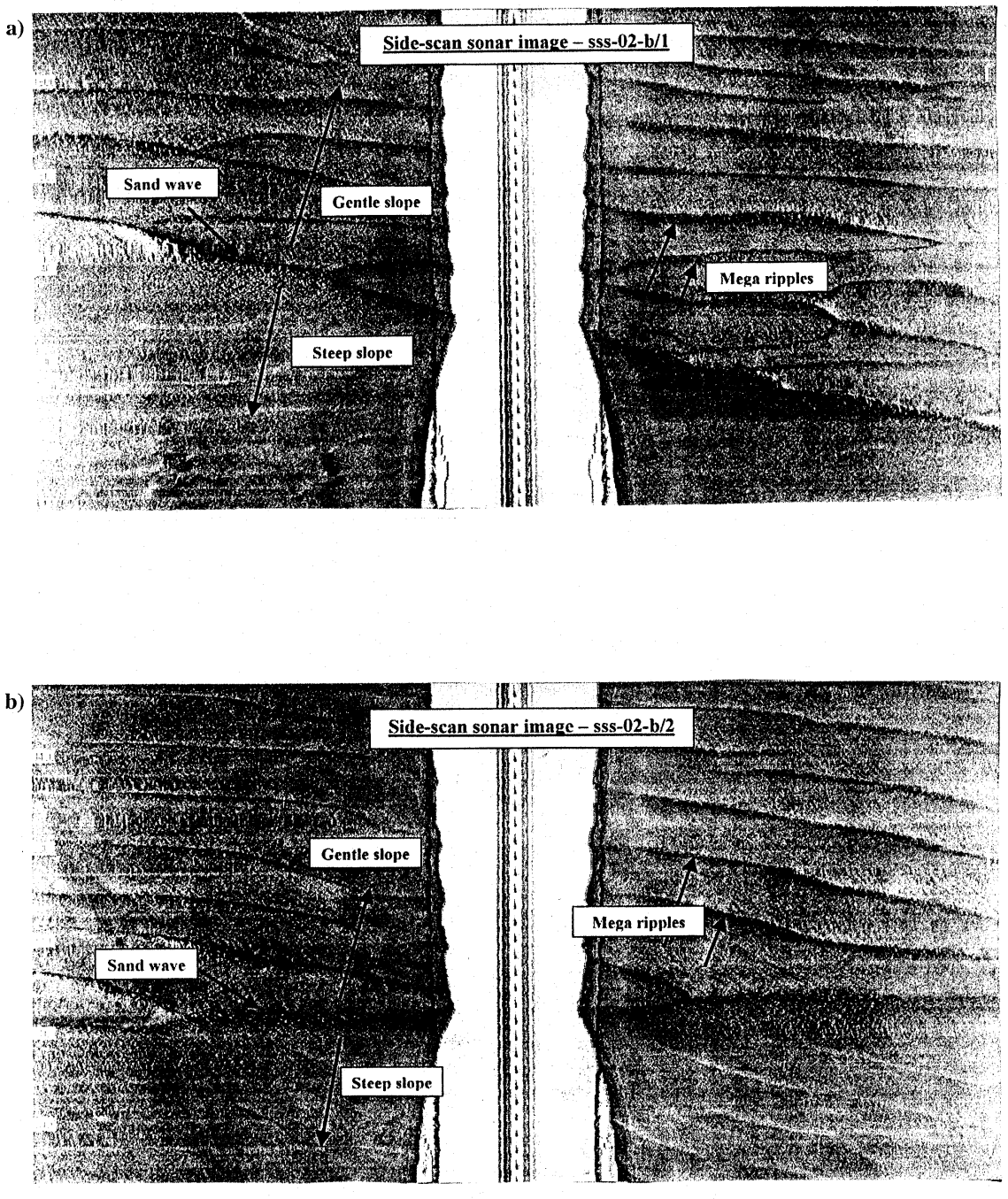

Fig. 2. Two selected side-scan sonar records a) sss-02-b/1 and b) sss-02-b/2 of the 500 kHz side-scan sonar system Klein 595 are shown taken at peak ebb tidal current velocity in southwesterly directions on April 08, 1997, between 09.01 UTC and 09.15 UTC (for location see Fig. 1).

2-Drift buoy, ADCP, and E-SAR NRCS data

During the main field experiment of the C-STAR project in April 1996 an Air-Sea Interaction Drift Buoy (ASIB) system was equipped with special sensors and instruments to measure the position of the buoy, the local water depth, the surface current velocity, the modulation characteristics of short waves, and relevant air-sea interaction parameters. Fig. 3 shows an example of the wind speed and direction, mean wave direction at 2 Hz (corresponding to P-band radar Bragg waves), surface current direction, and water depth for track 9 (for position see Fig. 1) taken on April 16, 1996. The mean wind speed was 4.3 m/s with south to southwesterly wind

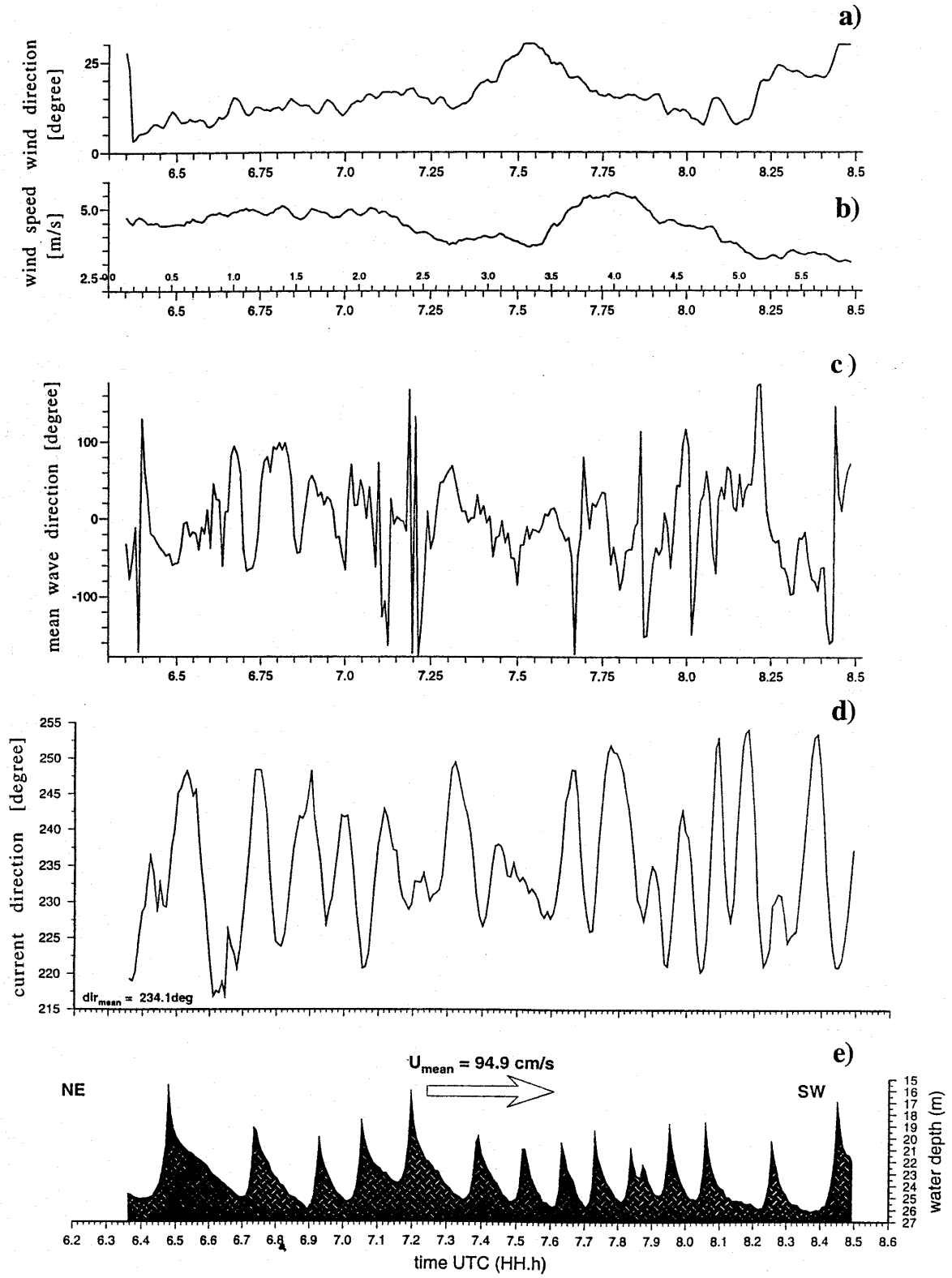

Fig. 3. Time series of a) wind direction, b) wind speed, c) mean wave direction at 2 Hz, d) surface current direction and e) water depth of track 9 on April 16, 1996.

directions. The wind vector shown in Fig. 3a is converted to the vector "going to". The mean wave direction presented in Fig. 3c also denotes the vector "going to". Negative values counting anticlockwise from 0^0 or 360^0. The mean wave direction of -100^0, for example, corresponds to $360^0 - 100^0 = 260^0$. A mean surface tidal current velocity of 0.95 m/s was measured over the time span of two hours by the Global Positioning System (GPS) on board the buoy. The measurements were performed around maximum ebb current. An electromagnetic current meter of less than 0.1 s time constant (Marsh McBirney, Inc., Gaithersburg, Model 511) was mounted on a small wave follower measuring surface currents at about 5 cm water depth. The currents result from current differences at the surface and at 1 m water depth which are dominated by the wind-induced surface drift. The absolute surface current velocity was calculated by using the GPS measurements on board the ASIB system. The direction of the tidal current was southwesterly. The wave energy density spectra and the mean wave direction are calculated over 32 s intervals from resistance wire data sampled at 128 Hz. Noise in the spectra was reduced by line fitting the short wave log-decay in the 0.8 - 10 Hz spectral range. From the fitted spectra the wave energy density was extracted at fixed frequencies as time series of 32 s resolution corresponding to about 30 m spatial resolution (at a tidal current of $1 ms^{-1}$). The measurements shown in Fig. 3 also indicate changes of the mean wave direction of short gravity waves with a frequency of 2 Hz by variations of the tidal current direction due to large sand waves.

An example of Acoustic Doppler Current Profiler (ADCP) measurements on board R.V. Planet from run 9 at 0616 - 08.31 UTC 16 April 1996 is shown in Figs. 4a-b. The depth averaged current velocity (Fig. 4a) and the water depth (Fig. 4b) are plotted as function of time. Only such depth cells (bins) were considered for the calculation which covered the depth range between 8.5 m water depth and 85 % of the total water depth. A mean current velocity of $U_{mean} = 70.2 cms^{-1}$ was calculated from the measurements. It can readily be noticed from Fig. 4 that all sand waves cause significant changes between 5 cms^{-1} and 18 cms^{-1} in the depth averaged current velocity. A clear anti-correlation was found between the current velocity and the water depth record. Maximum current velocities were observed at the crests of sand waves and minimum current velocities were calculated from the measurements at the troughs of sand waves. These measurements show that the tidal current behaviour must be traced from the near sea bed through the water column to the water surface.

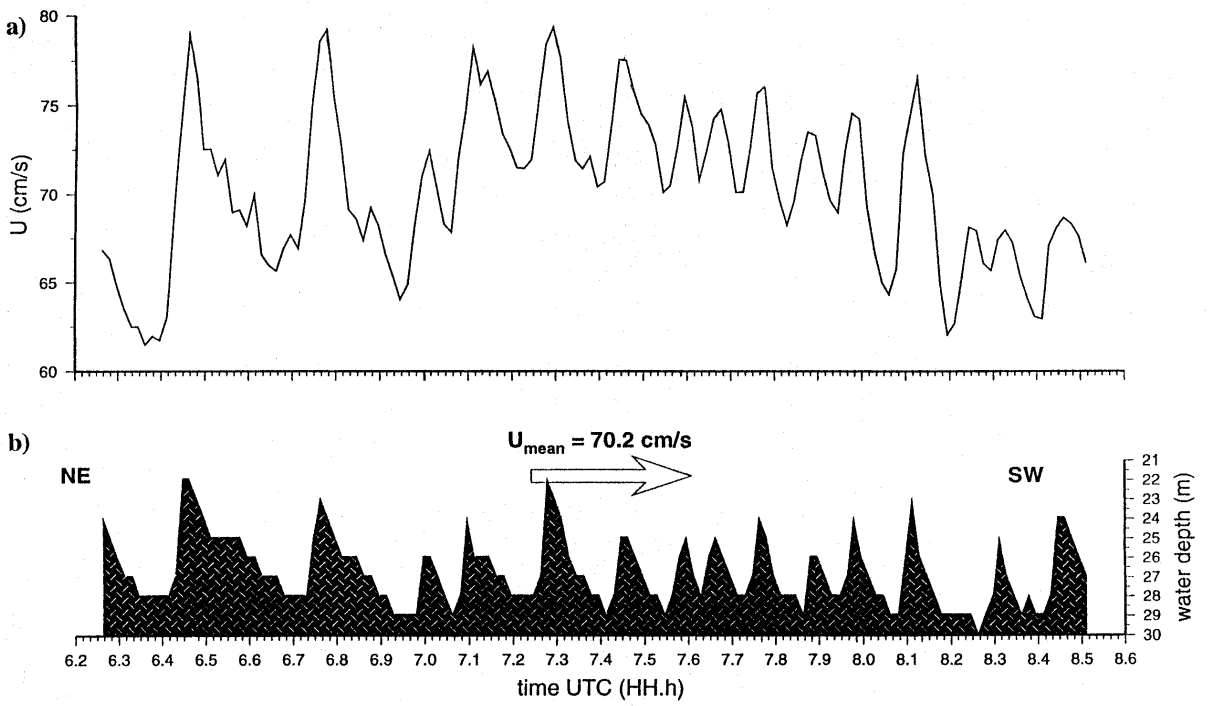

Fig. 4. Example of ADCP measurements performed on board R.V. Planet during southwesterly tidal current flow direction from run 9 at 0616 - 0831 UTC 16 April 1996; a) depth averaged current velocity and b) water depth as function of time.

The direction of short waves is mainly influenced by the local wind direction if there is no swell present but can also be changed significantly by convergent, divergent and shearing currents. A possible explanation of current direction variations according to Terwindt (1971) is that during times of large sand transport the direction of the flow over the sand wave forms an angle with the sand wave crest, generating a bending of flow lines (see section 2). The resulting current shear produces a torque that also changes the direction of the angular momentum of short waves along their rays (Kenyon and Sheres, 1996). Horizontal gradients in tidal currents caused by bottom topography in shallow water also affect the short wave amplitudes. Thus variations of the wave direction, directional spread and amplitude result from changes in tidal current speed and direction caused by bathymetric steering.

In situ measurements of the wave energy density spectrum modulation, the water depth, the surface current and direction, and the wind speed and direction derived on board the drift buoy as well as the P-band Normalized Radar Cross Section (NRCS) variation of the Experimental-Synthetic Aperture Radar (E-SAR) image acquired by the Deutsches Zentrum für Luft- und Raumfahrt (DLR), Oberpfaffenhofen, Germany, are shown in Fig. 5. The wave energy density is normalized with the mean value over the complete track, which is assumed to represent the equilibrium wave energy density for the present wind condition (mean wind speed of 4.3 ms^{-1}). The wave energy density was chosen at 2 Hz, as it corresponds to P-band Bragg waves of 0.44 m, which mainly contribute to the radar backscattering. The NRCS profile of the SAR image is averaged in sand wave direction over 50 m at both sides of the buoy track.

As indicated from the buoy measurements the reduced wave energy density regions correspond to the steep slope at the upstream (northeast) side relative to the sand wave crests, where strong current divergence due to decreasing water depth is expected. The correlation of wave energy density with bottom topography is obvious in most parts along the track. The reduced backscatter regions in the NRCS profiles of the SAR image are even more pronounced: the NRCS bands are smaller (30-60 m) and the modulation depth (typically 3-4 dB, minimum to maximum) is larger than for wave energy density (typically 2 dB). Despite some noise in both profiles and the lower spatial resolution of the wave energy density, both profiles compare well with respect to

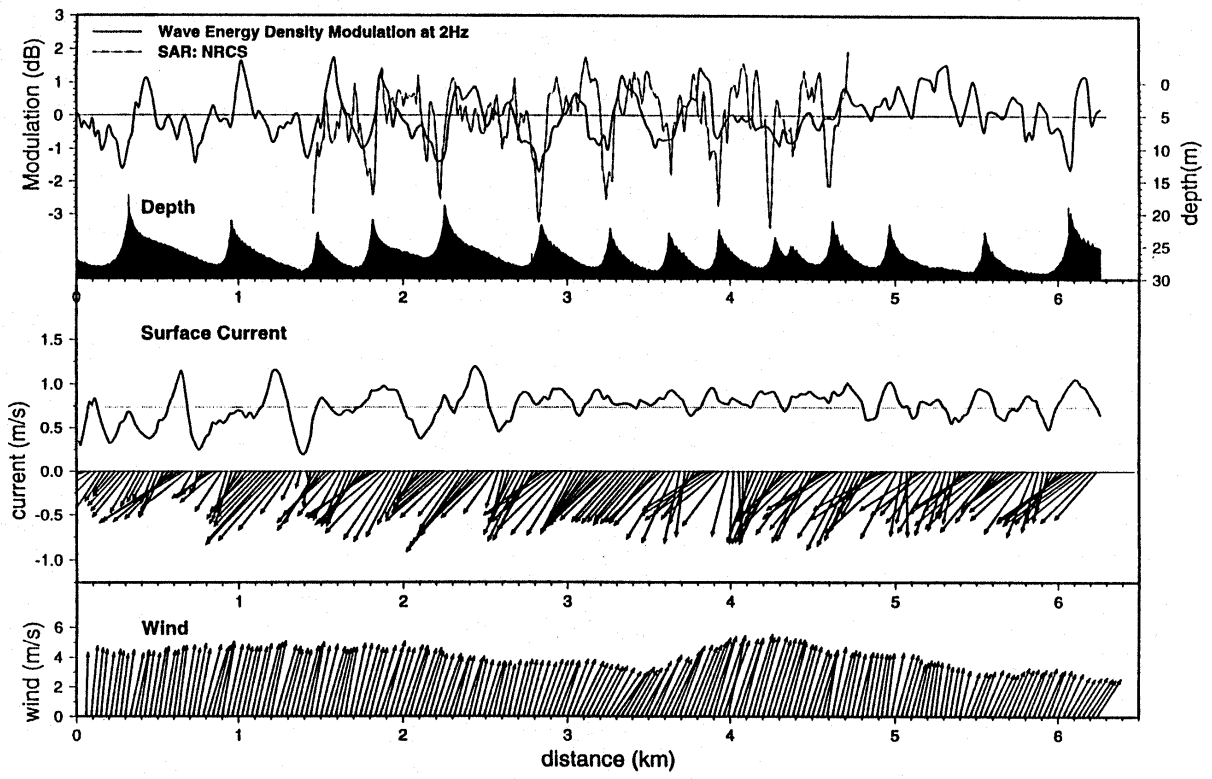

Figure 5. In situ measurements performed along the drift buoy track (for location see Fig. 1) at 0620 - 0830 UTC 16 April 1996. Top: wave energy density modulation at 2 Hz, NRCS modulation of E-SAR image, water depth (from echo sounder). Middle: Surface current (speed and vector). Bottom: wind.

the position of minima and maxima and the overall shape. The surface current in most cases changes direction when crossing the wave crests, whereas the current acceleration in the steep slope regions of the sand waves is often masked by the general current variability.

Summary and conclusion

One of the most significant new discoveries from radar imagery such as SEASAT Synthetic Aperture Radar (SAR) images, especially from a sedimentological point of view, was that the angle between tidal current ridges and maximum current velocity varies between 10^0-20^0 due to the presence of parallel roughness streaks on the sea surface induced by tidal currents. Such observations can be considered as somewhat analogous to explaining the tidal flow behaviour across sand waves using the orientation of megaripples for the purpose of predicting local sand transport paths (Lanckneus et al., 1994). For the prediction of streamlines, only the orientation of megaripple crests in relation to the sand wave crest has to be known. Although 30 years ago surface expressions of bathymetry were discovered in radar imagery of the sea there was still a need for experimental quantification to explain the coherent imaging mechanisms. A step forward was realized within the C-STAR project by collecting fundamental data of relevant hydrodynamic processes in the southern North Sea using a side-scan sonar and a special buoy system which drifted across large sand waves.

According to the results of the measurements derived by the side-scan sonar and the ASIB system it can be summarized that the variation of the direction of short and moderate water waves as well as changes of the tidal current direction across large sand waves must be considered for correct modelling of the wave-current interaction mechanism.

Acknowledgments. S. Stolte jun., S. Stolte sen., J. Förster, W. Waeber, H.-P. Westphal, and the captains and crews of the research vessels Planet and Belgica are gratefully acknowledged for their excellent cooperation and assistance during the project. We thank M. Metzner for technical support. This work has been supported by the European Community (EC) as a part of the Marine Science and Technology (MAST) programme under contract MAS3-CT95-0035 (C-STAR).

Reference:

Alpers, W. and Hennings, I., 1984. A theory of the imaging mechanism of underwater bottom topography by real and synthetic aperture radar. *J. Geophys. Res.* **89**, 10529-10546.

De Vriend, H.J., 1997. Evolution of marine morphodynamic modelling: Time for 3-D? *Dt. Hydrogr. Z.* **49**, 331-341.

Field, M.E., Nelson, C.H., Cacchione, D.A. and Drake, D.E., 1981. Sand waves on an epicontinental shelf: Northern Bering Sea. *Mar. Geol.* **42**, 233-258.

Hennings, I., 1998. An historical overview of radar imagery of sea bottom topography. *Int. J. Remote Sensing.* **19**, 1447-1454.

Houbolt, J.J.H.C., 1968. Recent sediments in the southern bight of the North Sea. *Geol. Mijnbouw*. **47**, 245-273.

Kenyon, K.E., and Sheres, D., 1996. Angular momentum and action in surface gravity waves: Application to wave-current interaction. *J. Geophys. Res.* **101**, 1247-1252.

Langhorne, D.N., 1973. A sandwave field in the Outer Thames Estuary, Great Britain. *Mar. Geol.* **14**, 129-143.

Lanckneus, J., De Moor, G. and Stolk, A., 1994. Environmental setting, morphology and volumetric evolution of the Middelkerke Bank (southern North Sea). *Mar. Geol.* **121**, 1-21.

McLeish, W., Swift, D.J.P., Long, R.B., Ross, D. and Merrill, G., 1981. Ocean surface patterns above sea-floor bedforms as recorded by radar, southern bight of North Sea. *Mar. Geol.* **43**, M1-M8.

Shuchman, R.A., Lyzenga, D.R. and Meadows, G.A., 1985. Synthetic aperture radar imaging of ocean-bottom topography via tidal-currents interactions: theory and observations. *Int. J. Remote Sensing.* **6**, 1179-1200.

Van Veen, J., 1935. Sand waves in the Southern North Sea. *Hydrogr. Rev.* **12**, 21-29.

Vogelzang, J., Wensink, G.J., Calkoen, C.J. and Van der Kooij, M.W.E., 1997. Mapping submarine sandwaves with multi-band imaging radar 2. Experimental results and model comparison. *J. Geophys. Res.* **102**, 1183-1192.

Terwindt, J.H.J., 1971. Sand waves in the southern bight of the North Sea. *Mar. Geol.* **10**, 51-67.